Chapter 4

Tomographic velocity estimation

4.1 Introduction and overview

The goal of processing seismic reflection data is to convert a recorded wave field into a structural or lithological image of the subsurface. Among the many steps in seismic processing, the imaging step, migration, not only positions, but also focuses reflector images. Migration requires a model of the wave propagation velocities of the subsurface, but obtaining this model is often the most difficult processing step in areas of complex structure.

In areas with structurally complex geology, conventional velocity analysis based on the stacking velocity (Taner and Koehler, 1969; Neidell and Taner, 1971) often fails. Consequently a more accurate velocity estimation scheme such as seismic tomography is required. Seismic tomography is an iterative two-step process. First, traveltime errors are measured by comparing observed traveltimes with computed traveltimes through an assumed velocity model. Then the differences are projected back over the traced ray paths through the assumed velocity model to update the model.

There are many different algorithms in tomographic velocity analysis, which can be characterized according to the domains they used for traveltime error picking. Conventional traveltime tomography (Bishop et al., 1985; Stork, 1988) picks the traveltime errors in the prestack data. Perhaps the greatest drawback of traveltime tomography of this type is the necessity for large amounts of picking. Events in seismic data are generally complicated and variable wave patterns; reducing this information to isolated time picks can involve large amounts of human judgement and can be very time consuming. The picking process is subject to systematic errors caused by ambiguities in defining events or by incorrect assumptions about the wavelet phase, as well as random error. Automatic picking programs can work faster than people, but human judgement is usually better at avoiding egregious mispicks. To increase the reliability of the picking, Biondi (1990) used the measurement of moveouts in the beam stack domain.

In order to reduce the number, errors, and bias of picking, we can use the semblance velocity stack panel for picking (Toldi, 1985). Since a pick of the best stacking velocity corresponds to a pick of the best-fitting hyperbolic traveltime for an event in the common-midpoint (CMP) domain, it can be interpreted as a filtered version of prestack traveltime picking (Fowler, 1988).

The results of those two types of the time domain picking can be achieved similarly in the image domain after prestack migration by picking events for every offset (van Trier, 1990) or by picking the best residual moveout (RMO) velocity along the events in the stacked images (Al-Yahya, 1989; Etgen, 1990). In contrast to transmission tomography, where ray endpoints are known, in reflection tomography the reflector positions are unknown, and an incorrect guess about them may lead to errors in velocity estimation. Picking in the image space, either event picking or RMO velocity picking, after prestack migration has the advantage of providing an accurate reflector location under the assumed velocity.

Tomographic velocity inversion constitutes a nonlinear inversion problem because both the velocity and ray paths are unknown. To solve such a nonlinear problem, we use a bootstrap approach. First, starting with an initial guess of the velocity model and the operator based on it, the traveltime errors are measured by comparing observed traveltimes with the computed traveltimes obtained through the assumed model. Next, the error in the assumed model is solved by inverting the measured traveltime errors and is used for updating the velocity model. We then iterate this linear inversion with the updated velocity model until it converges.

If we choose the RMO velocity analysis for traveltime error measure, a model-dependent RMO velocity analysis is required to compute accurate traveltime error. However, the measuring of the RMO velocity for a nonflat reflector is often difficult and not practical to implement because it requires a line search in a prestack migrated image cube (Zhang, 1990). To avoid such exhaustive searching, Etgen (1990) applied residual dip moveout (RDMO) before RMO velocity analysis so that the common reflection events could be lined up in the common surface location plane in the image cube.

This chapter describes a new way of measuring RMO velocity that reflects traveltime errors along the ray paths where the event has moved, with the help of plane wave synthesis imaging along irregular reflectors. First I review the basic traveltime tomography algorithm along with specific problems in reflection tomography. Then I explain how wavefront synthesis along irregular reflectors is used to generate reflector-oriented common reflection point (CRP) gathers, which provide accurate residual velocity. Finally, I summarize the entire algorithm for velocity estimation and present some examples. Since the algorithm presented in this chapter requires manual picking of reflectors that is the most tedious and time consuming process, a simple synthetic dataset with few reflectors was used to describe the algorithm instead of the Marmousi dataset that contains too many reflectors.

4.2 Reflection tomography

Traveltimes are a line integral of the slowness along the ray path expressed as

$$t = \int_s w ds, \tag{4.1}$$

where w is the slowness along the ray path, and s is the arc length along the ray path. With the slowness field discretized into cells, the forward problem of the traveltime is expressed as

$$\mathbf{t} = L\mathbf{w}, \tag{4.2}$$

where $\mathbf{t}$ is a vector of traveltimes, $\mathbf{w}$ is a vector of slowness, and L is a matrix in which a row contains the path lengths of a ray in each cell. This forward problem is a nonlinear equation because the operator L depends on the slowness vector $\mathbf{w}$.

This nonlinear problem can be linearized by subtracting a reference problem and expressing the forward problem of the traveltime deviations from the reference model as follows:

$$\Delta\mathbf{t} = L_0\Delta\mathbf{w}, \tag{4.3}$$

where $\Delta\mathbf{t}$ is a vector of traveltime deviations predicted from the reference model, $\Delta\mathbf{w}$ is a vector of slowness deviations from the reference model, and L_0 is a matrix in which a row contains the path lengths in each cell of the ray traced through the reference model, $\mathbf{w}_0$.

For a given traveltime deviation, $\Delta\mathbf{t}$, the slowness deviation from the reference model, $\Delta\mathbf{w}$, is obtained by inverting equation (4.3) using the least-squares approach.

In order to solve the original nonlinear problem (4.2), the above linearized inversion is applied iteratively with the updated back projection operator L_i, which is obtained by ray tracing through the new reference slowness model

$$\mathbf{w}_i = \mathbf{w}_{i-1} + \Delta\mathbf{w}_{i-1} \tag{4.4}$$

until the traveltime deviations $\Delta\mathbf{t}$ become small enough; the subscript i represents the iteration number.

Therefore, traveltime tomography can be summarized as an iterative two-step process. First, traveltime deviations are measured by comparing picked traveltimes with expected traveltimes obtained through an assumed velocity model. Then the differences are projected back over the traced ray paths through the assumed velocity model to update the model.

In contrast to transmission traveltime tomography, in which computation of the operator L only requires a slowness model to trace rays, reflection traveltime tomography requires additional information about reflectors, such as the dip and location. Therefore, an image space after prestack migration that can provide both the reflector information and the traveltime deviation is a good choice for picking.

4.3 Measuring Δt

The first step in traveltime tomography is measuring traveltime errors. For a given reference velocity model and reflector geometry, one can calculate traveltimes from each source to each receiver. Then traveltime errors are calculated by comparing the picked event with calculated traveltimes. Therefore, event picking is a prerequisite for measuring traveltime errors.

4.3.1 Event picking

The domain for picking plays a major role in deciding the type of tomography algorithm. Different algorithms use different domains for picking, such as the time or the depth in prestack or poststack, respectively. Among these picking algorithms, I chose the algorithm that picks events in the stacked image after prestack migration, which requires a minimum number of picks and provides reflector information. The advantage of having reflector information in the method based on event picking in the depth domain is achieved by prestack migration. For this research, I used planewave synthesis imaging that synthesizes planewaves at the surface.

As an example, I have generated a synthetic data set with finite-difference acoustic modeling. Figure 4.1 shows the interval velocity model used to generate the synthetic data. To avoid surface-related multiples, an absorbing boundary is applied at the surface. The near-offset section of the synthetic prestack data set, Figure 4.2, shows that the surface-related multiples have not been generated.

As an initial guess for the velocity of the medium, a two-layer model, shown in Figure 4.3, is used, with water velocity for the top layer, because we can easily estimate the depth of the water bottom from the seismic data even in a real case.

In order to obtain a reference image to pick dominant reflectors, I apply surface-oriented planewave synthesis imaging. I synthesized thirty-one different incidence angles at the surface; the stacked image of them all is shown in Figure 4.4. Figure 4.5 shows the locations of the reflectors picked, with reflector numbers assigned along them.

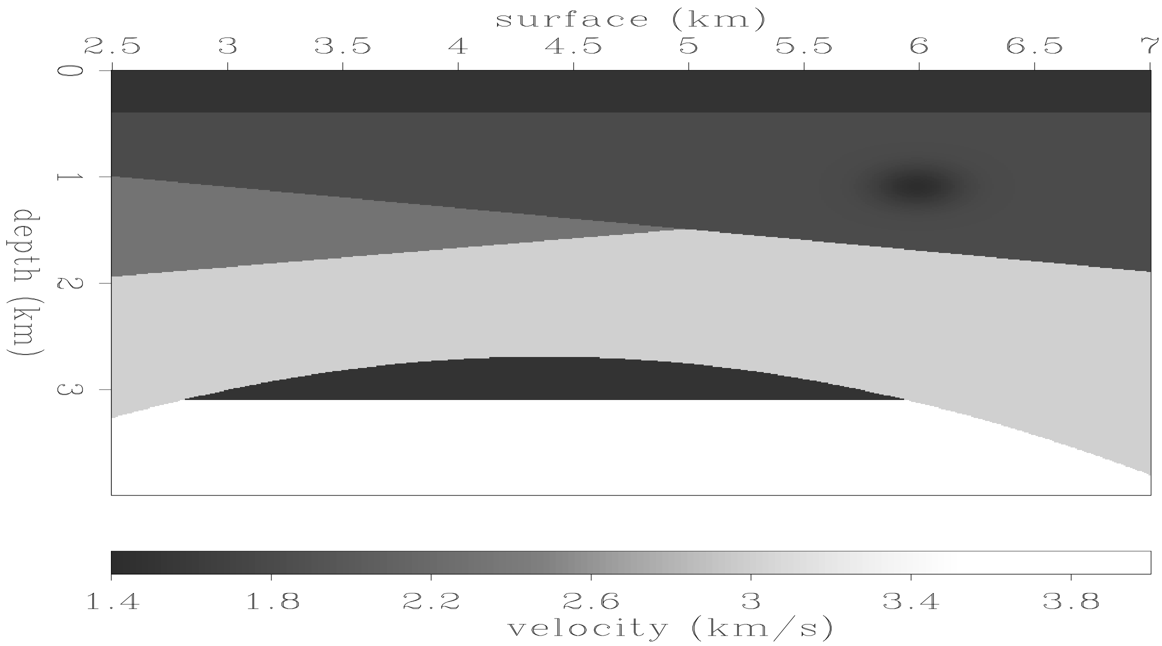

FIG. 4.1. Velocity model used to generate a synthetic data set with finite-difference acoustic modeling. tomovel-synvel [R]

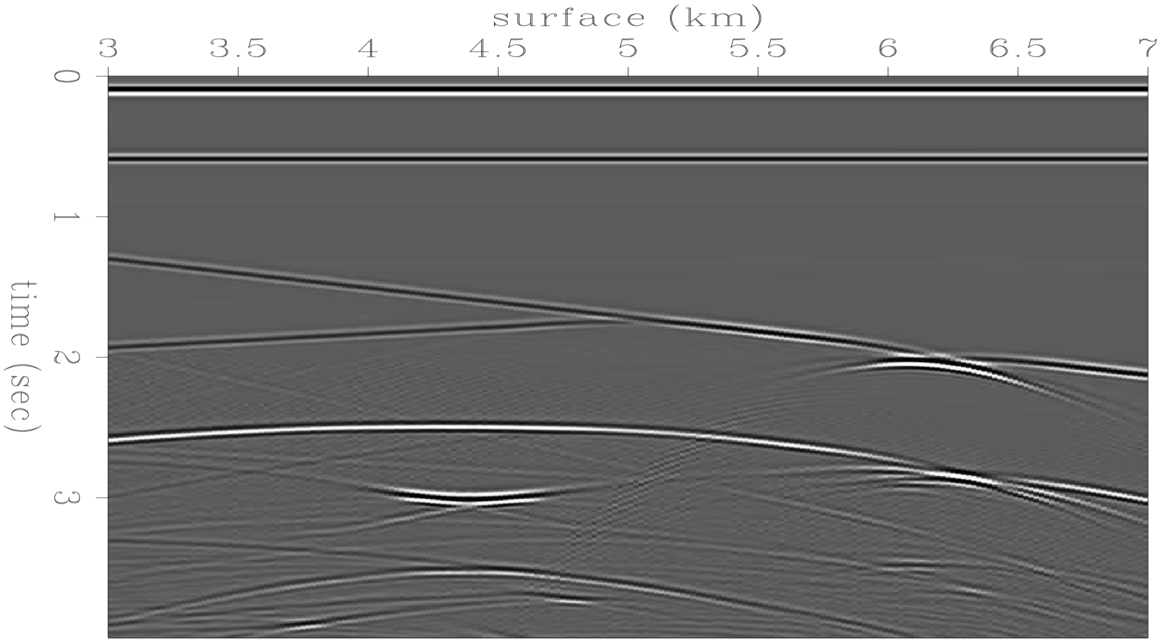

FIG. 4.2. Near-offset section modeled using the finite-difference method. tomovel-syn-near [R]

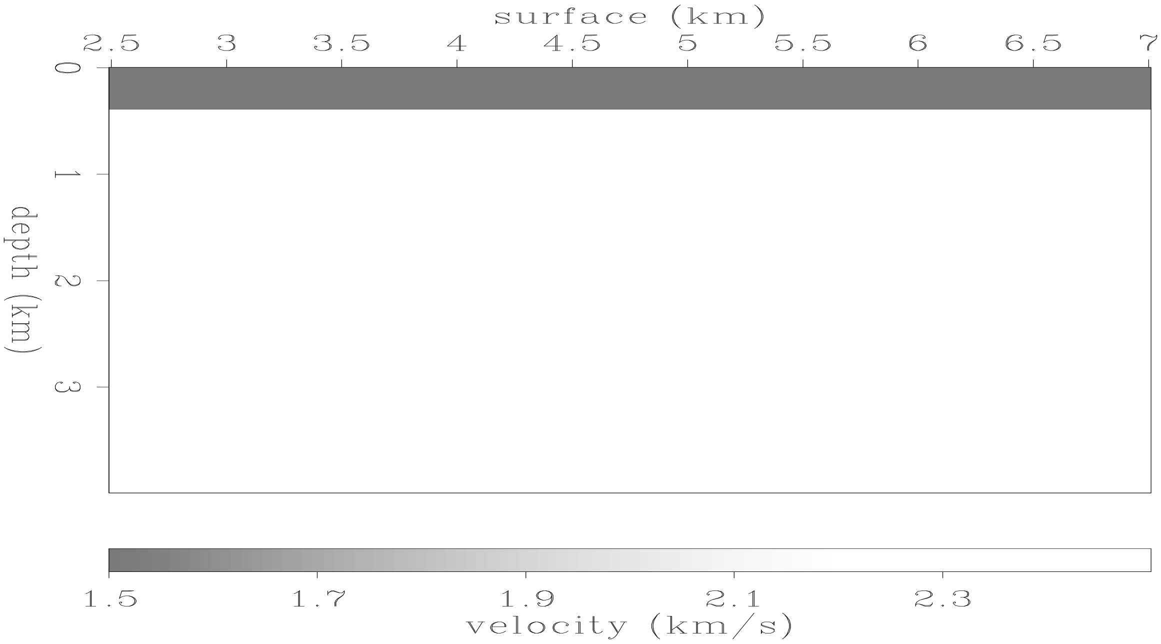

FIG. 4.3. Velocity model used as an initial guess. The top layer has a water velocity of $1500m/s$ with the same thickness as that of the true model, and the lower layer has a velocity of $2.5km/s$. tomovel-synvel-iter0 [R]

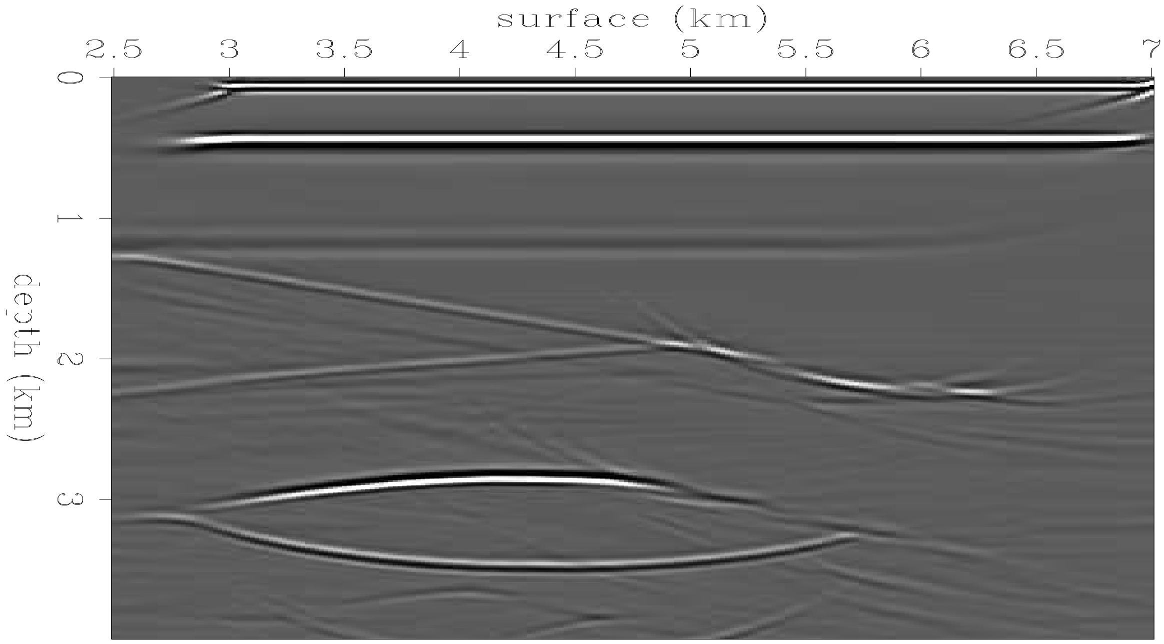

FIG. 4.4. Stacked image after planewave synthesis imaging that synthesized thirty-one different incidence angles, from -30 to +30 degrees, at the surface. tomovel-pws-syn-iter0 [CR]

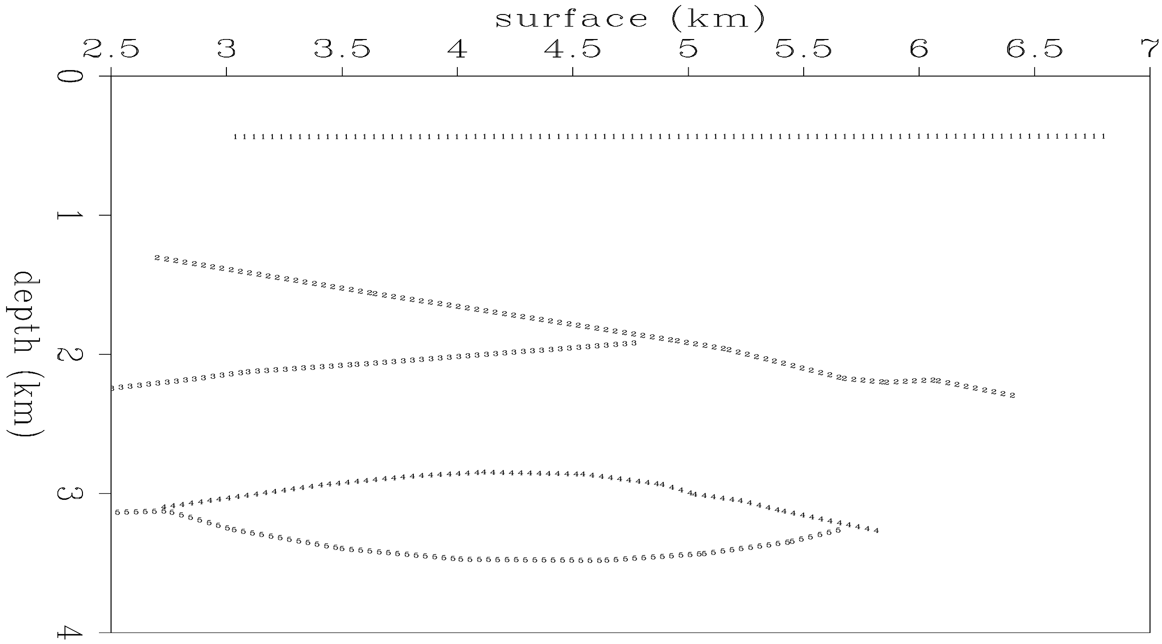

FIG. 4.5. The picked reflectors. The numbers along each reflector represent the reflector number assigned. tomovel-pick0 [R]

4.3.2 RMO velocity analysis

The computation of traveltime errors along the reflectors picked in the poststack image requires RMO velocity analysis. Measuring RMO implies relative movement of the reflection events in the common reflection point (CRP) gathers according to the different travel paths that each event follows.

Conventionally, RMO velocity analysis is performed in the common surface location (CSL) gather after prestack migration. The RMO velocity obtained from the CSL gather after prestack migration does not reflect the correct residual movement of CRP images because CRP images are not located in a CSL gather when a reflector has a dip. Therefore, we need to apply residual dip moveout (RDMO) before RMO velocity analysis of CSL gathers (Etgen, 1990) or else apply a dip-dependent RMO velocity analysis that is very difficult to implement or is not practical (Zhang, 1990).

Even though surface-oriented planewave synthesis imaging also shows residual moveout in CSL gathers, it is not easy to quantify in terms of residual velocity. This is because of the lack of the information about the implied ray trajectories. Since both the source and the received wave field used in planewave synthesis imaging are plane waves, we do not know which source and receiver locations correspond to an image. Therefore, we are forced to update the model qualitatively using the curvature of the RMO curves (Whitmore and Garing, 1993).

This drawback can be overcome by using reflector-oriented planewave synthesis imaging. With this method, the local incidence angle on top of the reflector is predefined. Thus, the image obtained can be interpreted as a wave field that follows the ray trajectory extended from the local incidence angle to the surface (Figure 4.6).

For example, I applied reflector-dependent planewave synthesis imaging for each reflector picked in the previous section (Figure 4.5). Figures 4.8 through 4.10 show some of the resulting CSL gathers. In contrast to the CSL gathers obtained from surface-oriented PWS imaging, each reflector image in the corresponding reflector-oriented PWS imaging shows a symmetric RMO pattern with respect to the normal incidence angle. The reason of the symmetric RMO pattern is that a ray that follows the shortest path from reflector to surface would have normal incidence angle to the reflector.

To quantify the residual moveout shown in the reflector-oriented PWS imaging, we can use the accurate dip-dependent RMO equation derived by Zhang (1990). However, the residual moveout equation is derived under the assumption that the medium above the

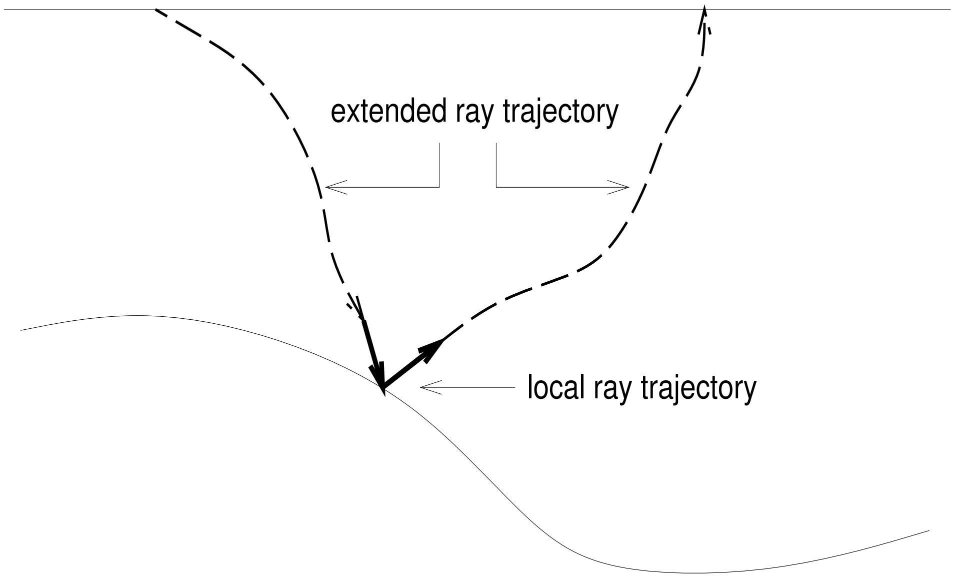

FIG. 4.6. Ray trajectory extended using the local incidence angel on top of a reflection point. tomovel-ray-extend [NR]

reflector has constant velocity and the ray trajectories are straight lines, which is not true when we are dealing with a variable-velocity medium. Therefore, for the convenience of velocity analysis, I derived a simplified RMO equation for a dipping event that resembles the RMO equation for a flat reflector.

Let us consider a dipping reflector as shown in Figure 4.12. The depth to a reflection point is z, the average slowness of the medium to the reflector is $\bar{w}$, and t is the recorded traveltime. If a planewave source has the incidence angle α to the reflector, the ray path from and to the reflector will be a straight line, and the presummed half offset h of the ray path can be approximately calculated from the incidence angle α of the planewave, the reflector depth z, and the dip of the reflector θ, as follows :

$$h = l \tan \alpha, \tag{4.5}$$

where $l = z/\cos(\theta)$ and represents the normal distance from reflector to the surface.

If we assume $n = m$ (see Figure 4.12), the traveltime is given by

$$t = 2\sqrt{h^2 + l^2} \cdot \bar{w}. \tag{4.6}$$

After migration with the slowness of the medium, the image under a surface location will be at the same depth z. If we migrate with an average slowness $\bar{w}_m$ instead of the slowness

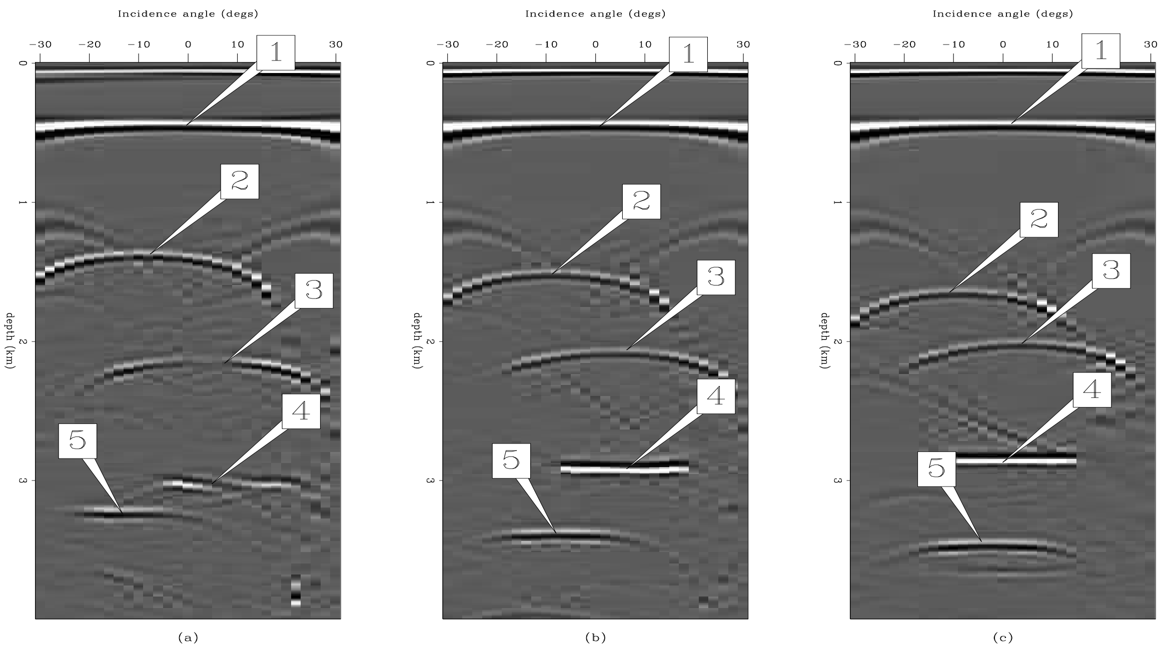

FIG. 4.7. Three CSL gathers at (a) 3 km, (b) 3.5 km, and (c) 4 km from the prestack image cube that was obtained by synthesizing plane waves at the surface. tomovel-crp-iter0 [CR]

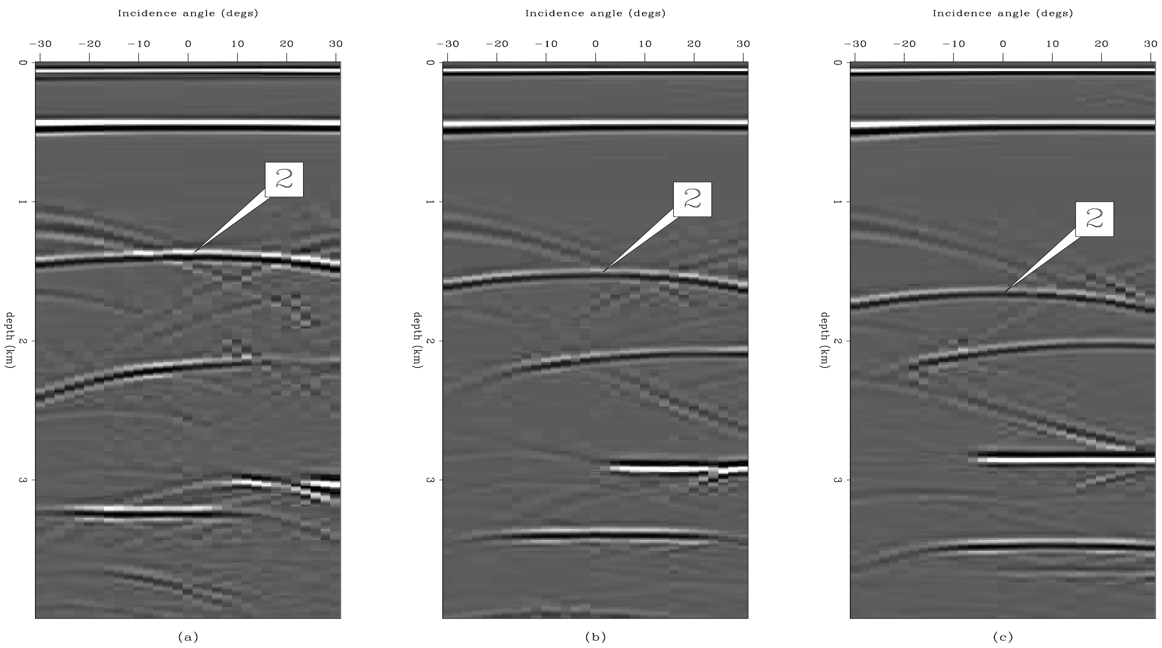

FIG. 4.8. Three CSL gathers at (a) 3 km, (b) 3.5 km, and (c) 4 km from the prestack image cube that was obtained by synthesizing plane waves at reflector number 2. tomovel-crp-iter0-2 [CR]

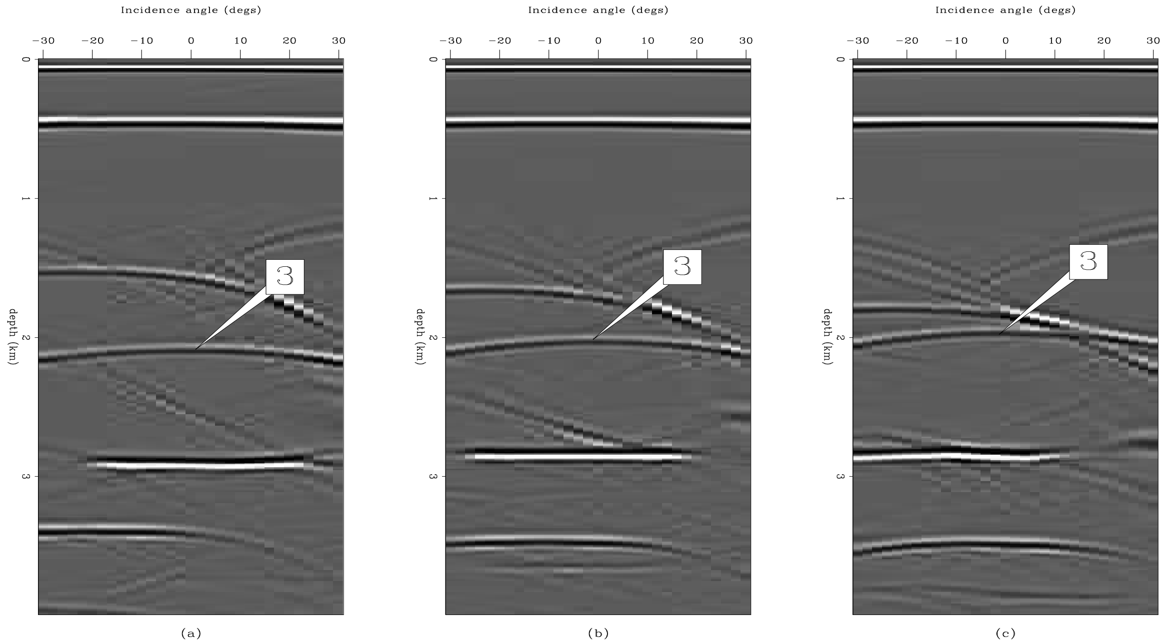

FIG. 4.9. Three CSL gathers at (a) 3 km, (b) 3.5 km, and (c) 4 km from the prestack image cube that was obtained by synthesizing plane waves at reflector number 3. tomovel-crp-iter0-3 [CR]

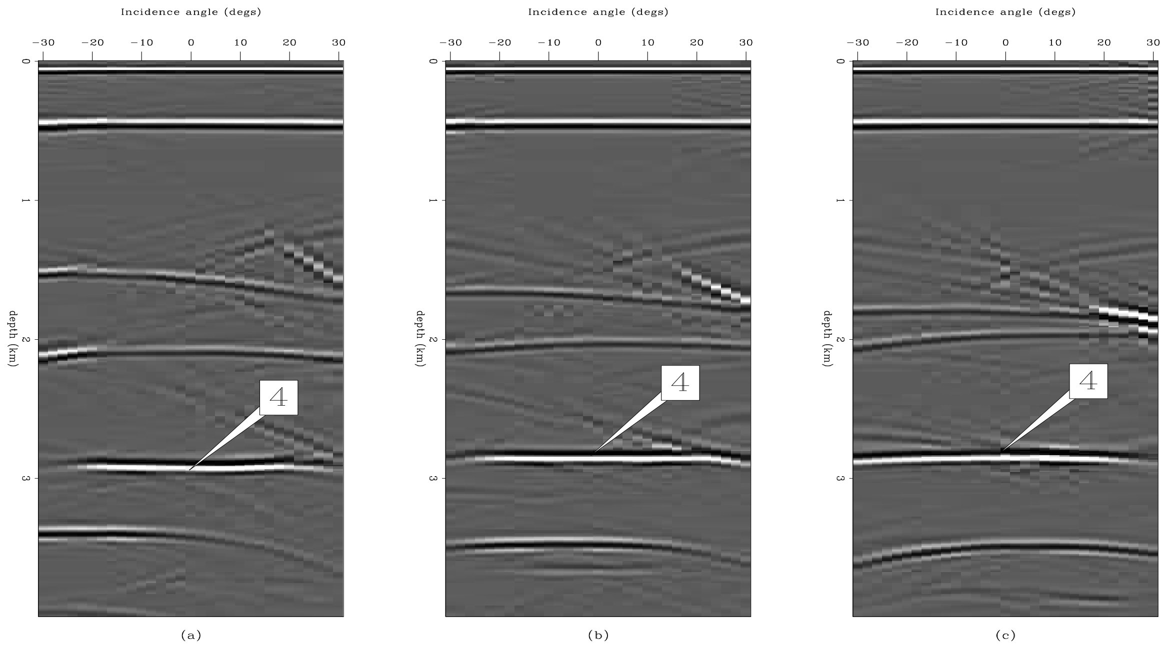

FIG. 4.10. Three CSL gathers at (a) 3 km, (b) 3.5 km, and (c) 4 km from the prestack image cube that was obtained by synthesizing plane waves at reflector number 4. tomovel-crp-iter0-4 [CR]

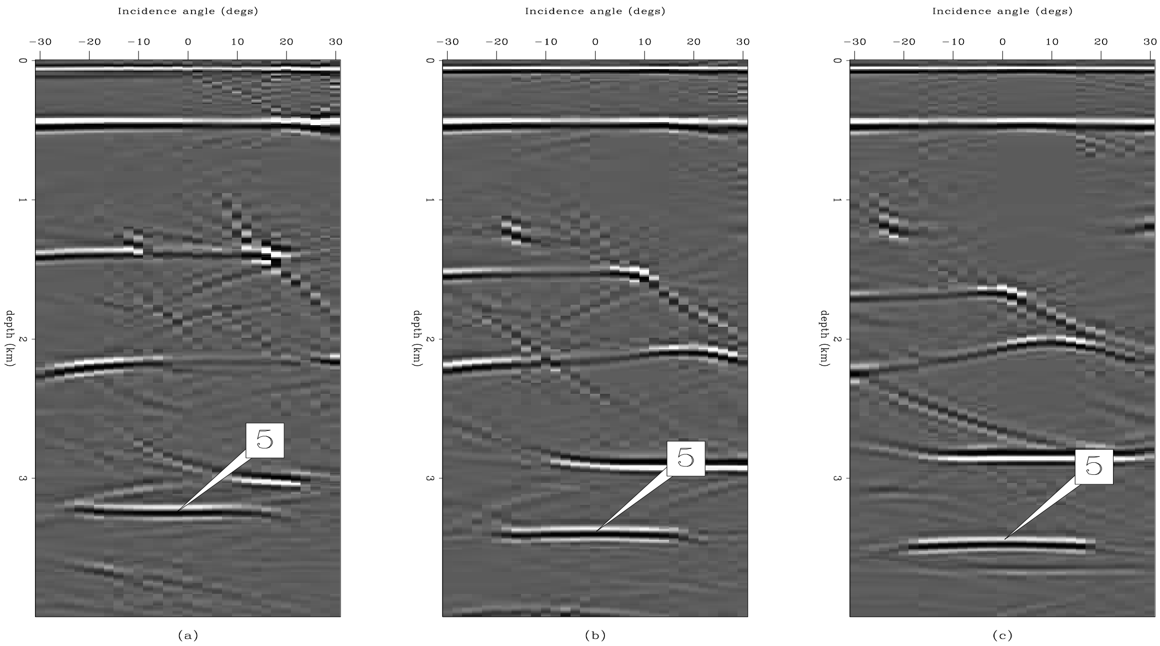

FIG. 4.11. Three CSL gathers at (a) 3 km, (b) 3.5 km, and (c) 4 km from the prestack image cube that was obtained by synthesizing plane waves at reflector number 5. tomovel-crp-iter0-5 [CR]

of the medium itself, the image under a surface location will be at depth z_m. In this case, the traveltime is given by

$$t = 2\sqrt{h^2 + l_m^2} \cdot \bar{w}_m, \tag{4.7}$$

where $l_m = z_m / \cos(\theta)$.

Note that the traveltime, t, is the same in equations (4.6) and (4.7) because it is an observed quantity. Eliminating t from equations (4.6) and (4.7), we obtain

$$z_m = \sqrt{\gamma^2 z^2 + (\gamma^2 - 1) h^2 \cos^2(\theta)}, \tag{4.8}$$

where

$$\gamma = \frac{\bar{w}}{\bar{w}_m}. \tag{4.9}$$

Equation (4.8) gives a relation between the apparent depth, z_m, and the actual depth, z. They are linked through the parameter γ. Note that they are equal regardless of the offset or incidence angle of the planewave when the slowness used in migration is equal to the slowness of the medium ($\gamma = 1$). This is the essence of the velocity analysis principle in the CSL gather; the image in a CLS gather is aligned horizontally if the velocity model

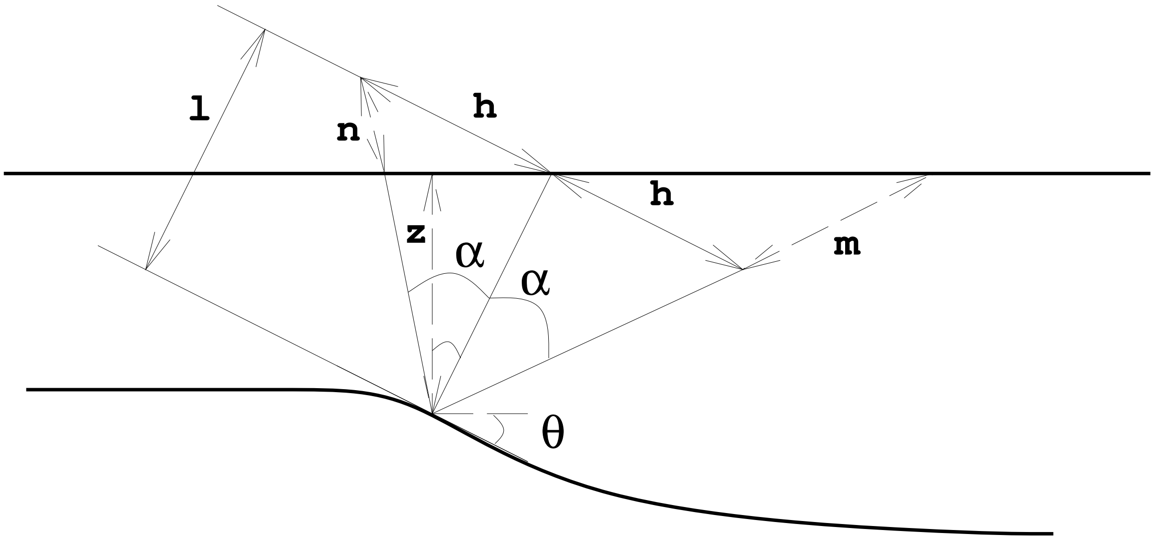

FIG. 4.12. For a reflector of dipping angle θ, a plane wave satisfies Snell's law. tomovel-crp-ray [NR]

is correct. When γ is not equal to 1, there is both a moveout as a function of offset and a shift at zero offset.

At each depth point along the reflector, RMO is defined by the parameter γ in equation (4.8). The data is then summed along this curved trajectory. The summation is done for a range of γ, and the sum is largest for the value of γ that matches the curvature. Because some signals may be weaker than others, the sum is normalized. This normalized summation is similar to the normalized summation along a hyperbola using the NMO equation, commonly known as semblance (Taner and Koehler, 1969). If the data in a CSL gather is $p(z_m, \alpha)$, then searching for curvature produces the semblance panel $g(z_m, \gamma)$, defined as

$$g(z_m, \gamma) = \frac{[\sum_\alpha p(z = \sqrt{z_m^2 + (\gamma^2 - 1)h(\alpha)^2 \cos^2\theta}, \alpha)]^2}{\sum_\alpha [p(z = \sqrt{z_m^2 + (\gamma^2 - 1)h(\alpha)^2 \cos^2\theta}, \alpha)]^2}. \tag{4.10}$$

Figure 4.13 shows that the semblance velocity analysis panel for the reflectors picked with γ values, which are the maximum semblance values for each CSL gather, are on top of semblance panel.

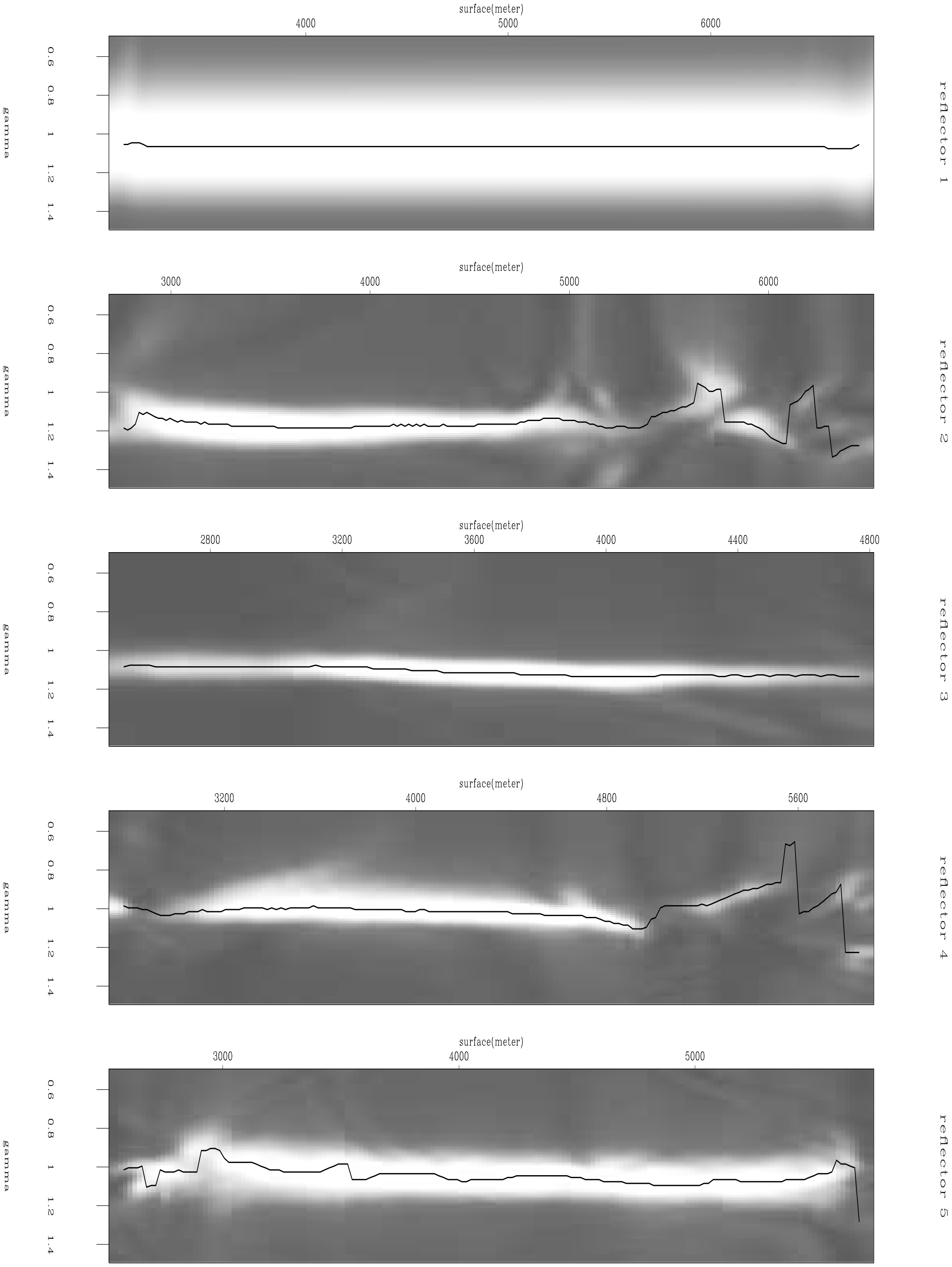

FIG. 4.13. Semblance stack panels for the picked reflectors. The γ values that correspond to the maximum semblance value are overlaid on top the semblance panel with lines. tomovel-velan-iter0 [CR]

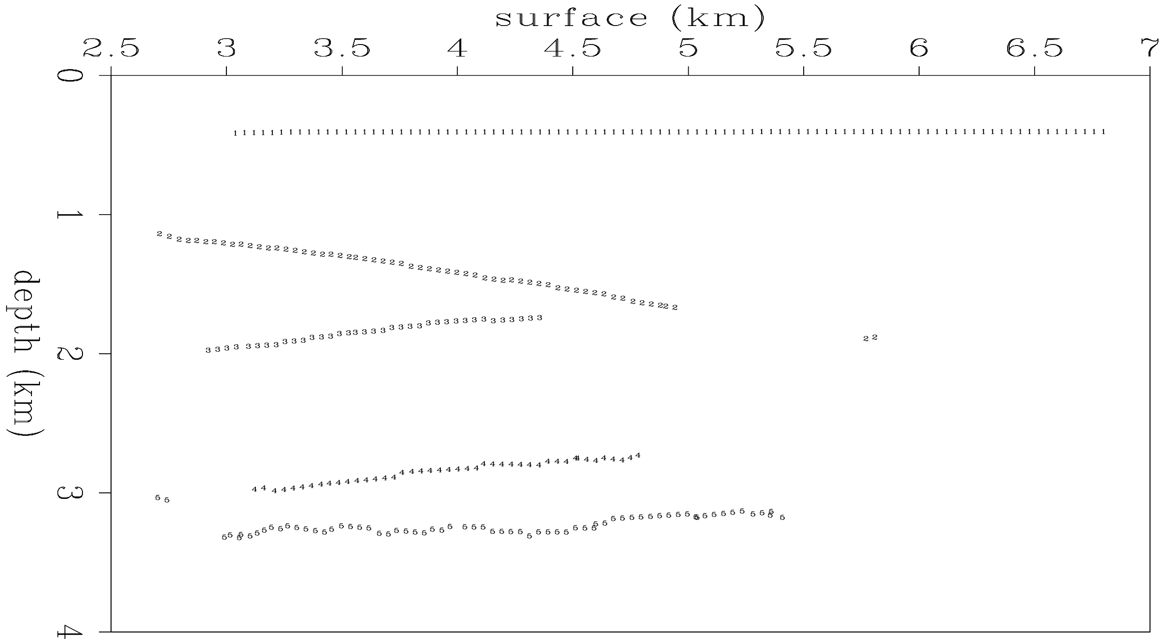

FIG. 4.14. The portions of the picked reflectors to be used for determining traveltime error. The reflector locations that have below .4 in semblance value were excluded in traveltime error calculation. tomovel-npick0 [R]

4.3.3 From γ to $\Delta\mathbf{t}$

The residual moveout velocity analysis, measuring γ, that was described in the previous section is an indirect way of measuring traveltime errors $\Delta\mathbf{t}$, which are required to compute the perturbation $\Delta\mathbf{w}$ in reference slowness as shown in equation (4.3).

The traveltime errors are the differences between the observed traveltimes $\mathbf{t_m}$ and the computed traveltimes $\mathbf{t}$ using an assumed slowness model

$$\Delta\mathbf{t} = \mathbf{t} - \mathbf{t_m}. \tag{4.11}$$

Both $\mathbf{t}$ and $\mathbf{t_m}$ are obtained by integrating slowness along the ray path traced through the assumed reference model,

$$\Delta\mathbf{t} = L(\mathbf{w} - \mathbf{w_m}), \tag{4.12}$$

and this is equivalent to an integration of average slowness as follows:

$$\Delta\mathbf{t} = L(\bar{\mathbf{w}} - \bar{\mathbf{w}}_m). \tag{4.13}$$

where $\bar{\mathbf{w}}$ and $\bar{\mathbf{w}}_m$ represent average slownesses of the true model and of the reference model, respectively.

By substituting $\bar{\mathbf{w}} = \gamma \bar{\mathbf{w}}_m$ into equation (4.13), we get

$$\Delta \mathbf{t} = L(\gamma - 1)\bar{\mathbf{w}}_m. \tag{4.14}$$

Therefore, we calculate $\Delta \mathbf{t}$ from the picked γ and average reference slowness along the the ray trajectory.

4.4 Calculating the slowness error $\Delta \mathbf{w}$

Calculation of the slowness error $\Delta \mathbf{w}$ by inversion of the traveltime error $\Delta \mathbf{t}$ requires that we first to find the back projection operator. The back projection operator L is found by ray tracing from reflector locations to the surface through the reference model.

The deviations of γ values from 1 mean that the reflector locations picked are not the correct reflector locations. To obtain more correct reflector locations to be used for ray tracing, reflector locations are corrected appropriately by using γ values as follows:

$$l_{new} = \frac{l_{old}}{\gamma} \tag{4.15}$$

where l_{old} represents the distance between the surface and the reflector drawn by a normal incidence ray to the reflector and l_{new} is the new adjusted distance along the same ray trajectory.

Some portions of the reflectors in Figure 4.13 have much lower semblance values than other portions. In order to avoid possible bias in inversion from this erroneous information, I excluded reflection locations that have semblance values below 0.4. The rest of the reflectors to be used in the inversion are shown in Figure 4.14.

4.4.1 A system of ray tracing equations

The ray tracing method I have implemented is based on the ray tracing system of first-order partial-differential equations, derived from the Eikonal equation by the method of characteristics (see Cerveny(1987) for more details):

$$\begin{aligned} \frac{dx_i}{ds} &= \frac{p_i}{w} \\ \frac{dp_i}{ds} &= \frac{\partial w}{\partial x_i} \end{aligned} \tag{4.16}$$

Here w is the slowness, $x_i = x_i(s)(i = 1, 2, 3)$ are the coordinates of the ray as a function of s, the arclength along the ray, and $p_i(s)$ are the components of the slowness vector $\bar{\mathbf{p}}$. The traveltime $t(s)$ along the ray is given by

$$\frac{dt}{ds} = w. \tag{4.17}$$

The slowness vector is perpendicular to the wavefront ($\bar{\mathbf{p}} = \nabla t$), and must satisfy

$$|\bar{\mathbf{p}}|^2 = \sum_{i=3}^{3} p_i^2 = w^2. \tag{4.18}$$

The system of ray equations together with equation (4.17) can be solved by a standard numerical integration method. I use a fourth-order Rungge-Kutta method. It propagates the properties of the ray (x_i,p_i, and t) over an increment in arclength by combining the information from several Euler-style steps (each involving one evaluation of the right-hand side of equations (4.16) and (4.17)), and then uses the information obtained to match a fourth-order Taylor series expansion of the ray variables at the current position.

Figure 4.15 shows some of rays traced through the reference model shown in Figure 4.3.

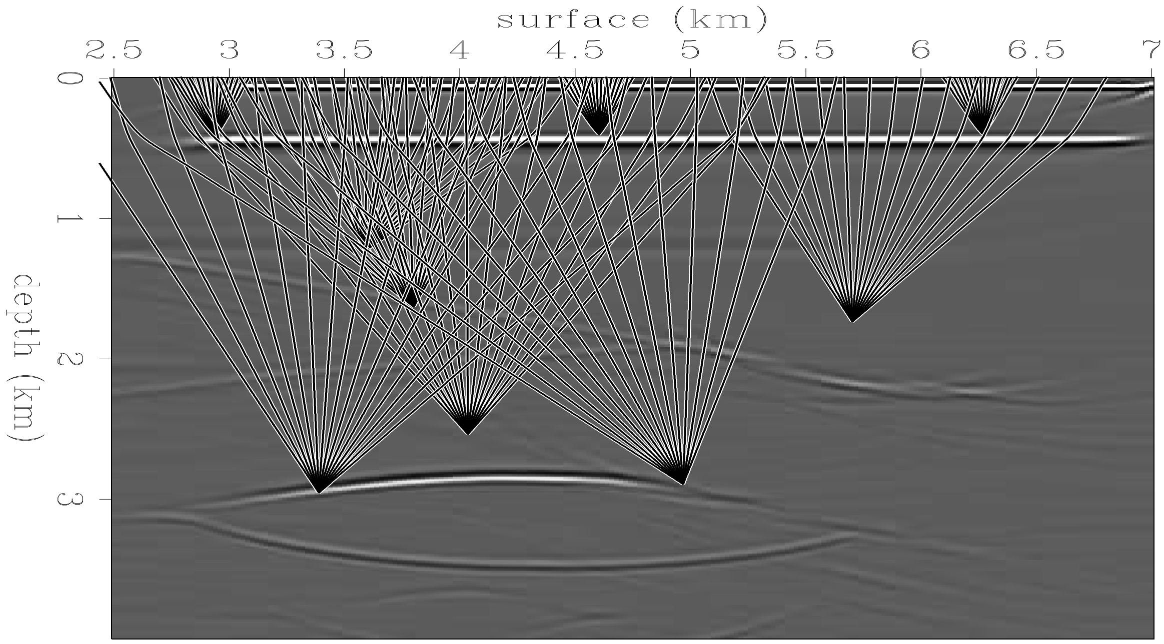

FIG. 4.15. Some of the ray trajectories traced through the reference medium to calculate the operator L. tomovel-ray0 [CR]

4.4.2 Model parameterization by spline

An accurate estimation of the gradient of the slowness field is necessary if we are to trace rays in a velocity model with high velocity contrast. Therefore, I have chosen to use cubic B-splines (Inoue, 1986) to parametrize the slowness model, which enables me to calculate the slowness gradient at an arbitrary point in the model. Another reason for using splines is that a wide variety of slowness models can be represented by a few spline coefficients. This means that the number of parameters in an optimization scheme that inverts for slowness can be reduced considerably.

The spline representation of a two-dimensional slowness model is

$$w(x_1, x_2) = \sum_{i=1}^{N}\sum_{j=1}^{M} c_{ij} F_i(x_1) G_j(x_2), \tag{4.19}$$

with N and M the number of spline knots in the x_1- and x_2-direction. F_i and G_j are the spline functions at the ith knot in the x_1-direction and the jth knot in the x_2-direction, respectively.

4.4.3 Inversion using the conjugate gradient method

After tracing rays and representing the slowness field with spline coefficients, the object function we want to minimize in the least squares sense is

$$J = (\Delta \mathbf{t} - LS\mathbf{c}), \tag{4.20}$$

where S is the spline function shown in (4.19), and $\mathbf{c}$ is a vector of spline coefficients. I used the conjugate gradient algorithm to solve the least squares problem (4.20). In using this algorithm, we do not need to construct the operator L in a matrix form, which is generally huge in size. Since summing slowness along the ray paths is the forward operation and putting the traveltime error along the ray paths is the adjoint of it, we only need to store the ray paths that correspond to nonzero components of the operator L.

After finding $\mathbf{c}$ for the measured traveltime error $\Delta\mathbf{t}$, the slowness error $\Delta\mathbf{w}$ is obtained from (4.19). Figure 4.16 shows the slowness field updated by the least-squares inversion of $\Delta\mathbf{w}$. Comparing it to the true velocity model Figure 4.3, we can see that the low-frequency component of the slowness field was found very easily even in one iteration.

Figure 4.17 is a stacked image after planewave synthesis imaging that synthesized 31 different incidence angles, from -30 to +30 degrees, at the surface, using the updated slowness model (Figure 4.16). Most of the reflectors are located closer to the real position than that of the images obtained using the initial reference model. And CSL gathers (Figure 4.18) show that most of the reflectors are almost lined up horizontally.

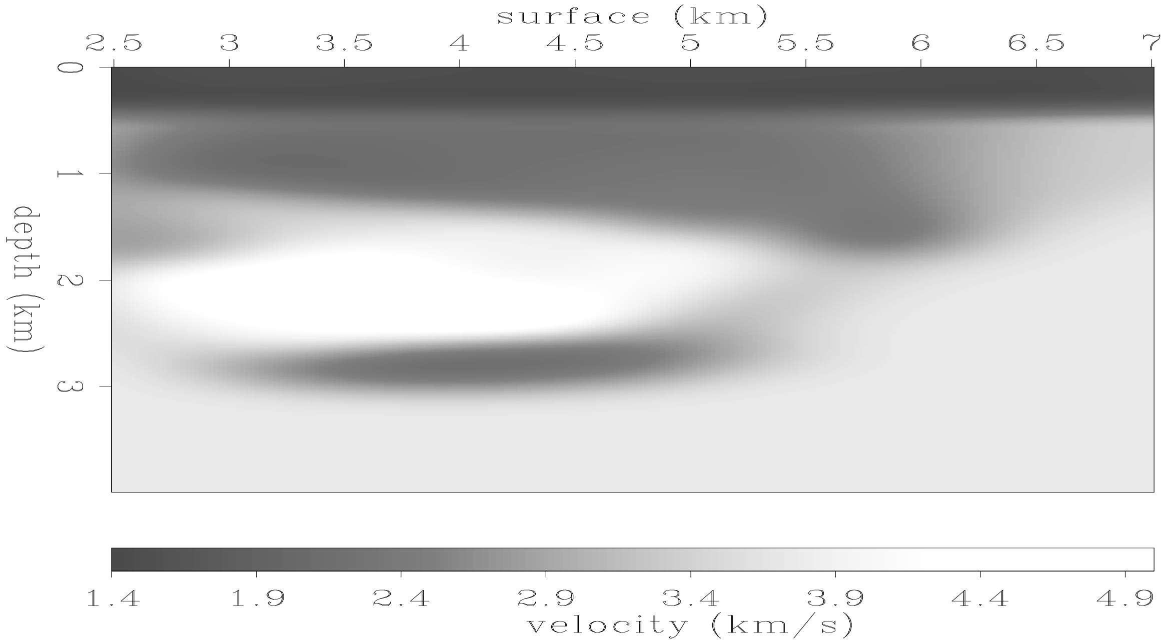

FIG. 4.16. Velocity model updated by adding Δw, which was calculated by inverting Δt, to the initial guess w. This corresponds to one iteration of the traveltime tomography inversion. tomovel-synvel-iter1 [CR]

4.5 Summary of the algorithm

The tomographic velocity analysis method with planewave synthesis imaging presented in this chapter can be summarized as follows:

- Define an initial model w.
- Begin Loop
  1. Event picking:
     - Perform surface-oriented planewave synthesis imaging.
     - Pick dominant reflectors in the stacked image.
  2. Measuring the traveltime error:

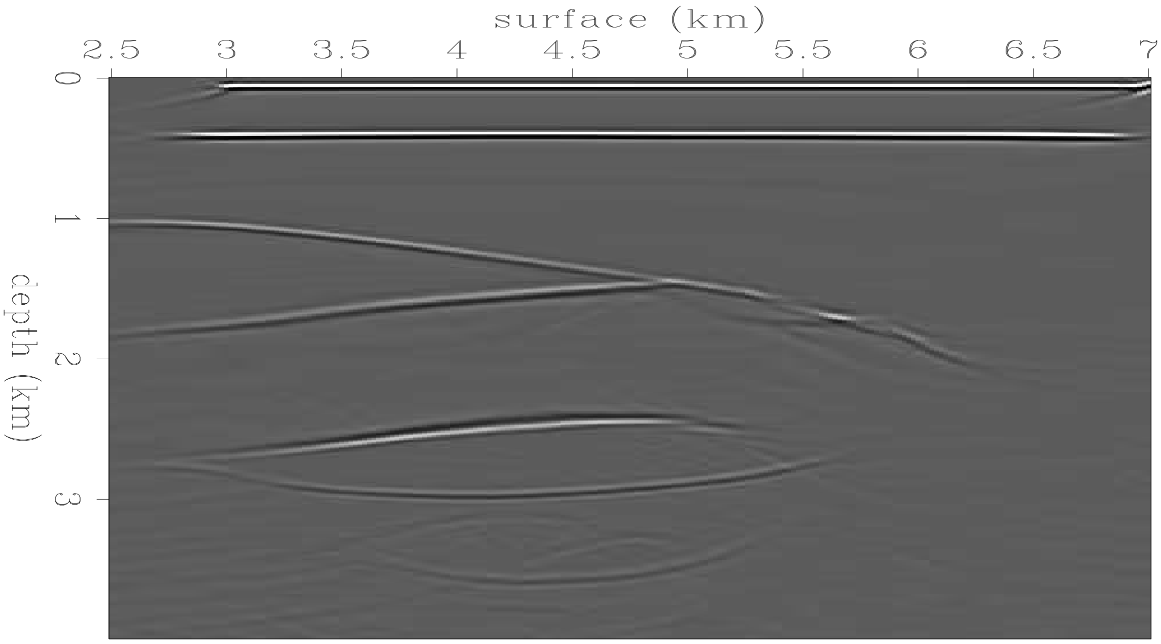

FIG. 4.17. Stacked image after planewave synthesis imaging that synthesized 31 different incidence angles, from -30 to +30 degrees, at the surface. For imaging, the updated velocity model (Figure 4.16) was used. tomovel-pws-syn-iter1 [CR]

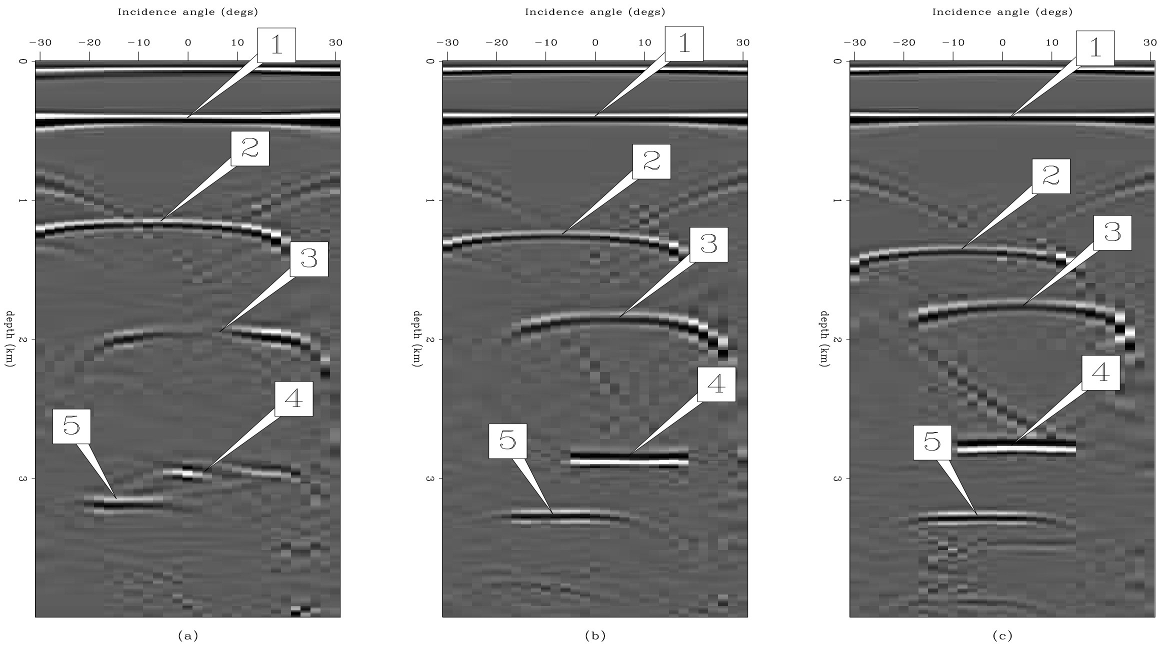

FIG. 4.18. Three CSL gathers at (a) 3 km, (b) 3.5 km, and (c) 4 km from the prestack image cube that was obtained by synthesizing plane waves at the surface using the updated velocity model (Figure 4.16). tomovel-crp-iter1 [CR]

- Perform reflector-oriented planewave synthesis imaging for each reflector.
- Do RMO velocity analysis for each reflector picked.
- Select γ based on semblance value.
- Convert γ to Δt.

3. Calculating the slowness error from the traveltime error:
   - Calculate Δw by inverting Δt using conjugate gradient.
   - Update $w = w + \Delta w$.
4. Convergence test: If Δw is small, exit from the loop.

- END Loop

4.6 Summary

This chapter has introduced a new tomographic velocity analysis method that uses planewave synthesis imaging. In order to measure traveltime error in the image domain after prestack migration, residual moveout (RMO) velocity analysis is performed in common surface location (CSL) gathers after reflector-dependent planewave synthesis imaging. Since the reflector-dependent planewave synthesis imaging provides symmetric RMO with respect to the normal incidence angle to the reflector, the measured RMO velocity contains more accurate traveltime error information than that of surface-oriented planewave synthesis imaging. The measured traveltime errors are inverted to determine the errors in the reference slowness in terms of spline parameters, using the conjugate gradient algorithm. The test of the algorithm for a synthetic data set shows fast convergence to a true slowness model even in only one iteration. The algorithm is also applied to a field data set and the result is shown in chapter 6.